J Solid State Electrochem (2007) 11: 339–349
DOI 10.1007/s10008-006-0142-y

ORIGINAL PAPER

M. Łukaszewski · A. Czerwiński

Electrochemical behavior of Pd–Rh alloys

Received: 15 December 2005 / Revised: 4 January 2006 / Accepted: 20 February 2006 / Published online: 23 March 2006
© Springer-Verlag 2006

Abstract Pd–Rh alloys were prepared by electrochemical codeposition. Bulk compositions of the alloys were determined by the energy dispersive X-ray analysis method, while surface compositions were determined from the potential of the surface oxide reduction peak. Cyclic voltammograms, recorded in 0.5 M H_2SO_4 for Pd–Rh alloys of different bulk and surface compositions, are intermediate between curves characteristic of Pd and Rh. The influence of potential cycling on electrochemical properties and surface morphologies of the alloys was studied. Due to electrochemical dissolution of metals, both alloy surface and bulk become enriched with Pd. Carbon oxides were adsorbed at a constant potential from the range of hydrogen adsorption. The presence of adsorbed CO_2 causes remarkable diminution of hydrogen adsorption but it does not significantly influence hydrogen insertion into the alloy bulk. On the other hand, in the presence of adsorbed CO, both hydrogen absorption and adsorption are strongly suppressed. Oxidative removal of the adsorbates results in a characteristic voltammetric peak, whose potential increases with the decrease in Rh surface content. Electron per site (eps) values calculated for the oxidation of the adsorbates change with alloy surface composition, more for CO_2 than CO adsorption, indicating the variation of the structure and composition of CO_2 and CO adsorption products. The course of the dependence of eps values on surface composition suggests that the products of CO_2 and CO adsorption on Pd–Rh alloys are similar but not totally identical.

M. Łukaszewski · A. Czerwiński (✉)
Department of Chemistry, Warsaw University,
Pasteura 1,
02-093 Warsaw, Poland
e-mail: aczerw@chem.uw.edu.pl
Tel.: +48-22-8220211
Fax: +48-22-8225996

A. Czerwiński
Industrial Chemistry Research Institute,
Rydygiera 8,
01-793 Warsaw, Poland

Keywords Pd–Rh alloys · CO_2 adsorption · CO adsorption · Cyclic voltammetry

Introduction

The electrochemical behavior of binary alloys of noble metals has been widely investigated [1–37], mainly in the context of their electrocatalytic properties. Among the systems studied, including Pt–Rh [1–10], Pt–Ru [4, 11–13], Pd–Pt [14–20], Pd–Au [1–3, 21–30], and Pt–Au [1, 21, 31–37] alloys, the Pd–Rh system belongs to rather rarely examined ones. Most research of Pd–Rh alloys has been devoted to the phenomenon of hydrogen absorption. This system is particularly interesting in that aspect because alloys containing small amounts of Rh can absorb more hydrogen than pure Pd [38–42]. However, the basic electrochemistry of Pd–Rh alloys has not been sufficiently explored and few such reports are available in the literature [1, 2, 4, 10].

Although Pd and Rh are neighboring elements in the periodic table, their electrochemical properties are markedly different, which is well reflected in different courses of cyclic voltammograms characteristic of those metals [1, 2]. Pd can absorb large amounts of hydrogen, while for Rh, bulk hydrogen dissolution is negligible [42]. On the other hand, both these metals are known to electrochemically adsorb hydrogen at potentials positive to the reversible hydrogen potential, i.e., underpotential deposition of hydrogen (UPD H) occurs on these materials [1, 43]. The elements also differ between each other in their electrochemical behavior at sufficiently high potentials where the oxidation of electrode material takes place. Surface oxide formation and reduction on Rh electrodes, as well as the beginning of the electrochemical dissolution of Rh, occur at potentials lower than on Pd [1, 44–46]. It should be mentioned that under certain conditions of a cyclic voltammetric experiment, the process of surface oxide reduction gives a well-defined peak whose potential is characteristic of a particular noble metal and varies linearly with surface composition in the case of homogeneous

binary noble metal alloys [1, 2, 16, 17], and this peak is utilized for in situ determination of surface composition of such electrodes.

Among the reactions investigated when the electrochemical behavior of alloy electrodes is examined are the processes of adsorption of small carbon-containing molecules, including carbon oxides. This subject is strictly linked to the constant search for new electrode materials for methanol fuel cells, in which various forms of adsorbed CO_2 and CO are the fuel oxidation products. It has been established that in acidic solutions, CO_2 adsorption on Pt and Rh takes place only at potentials from the hydrogen adsorption region [47–49], while CO can be adsorbed at potentials from both the hydrogen and double-layer regions [50–53]. In contrast to Pt and Rh, Pd electrode in acidic solutions is totally inert in CO_2 adsorption reactions at potentials positive to the reversible hydrogen potential [54, 55], despite the existence of UPD H on its surface. On the other hand, CO can be adsorbed on all platinum group metals, including Pd [50, 55]. The adsorption of CO_2 and CO is electrochemically irreversible; the potential of the adsorbate oxidative removal is much higher than the adsorption potential.

In the literature, there have been many reports on the nature of the product of CO_2 [49, 56–59] and CO [50, 52, 53, 60–63] adsorption on Rh electrodes in acidic solutions. However, there is still a controversy about whether CO_2 and CO adsorption products are identical or different [52, 53]. Although the authors generally agree on the presence of linearly and bridge-bonded CO species, other adsorbates have also been postulated in the literature, namely, a reduced form of adsorbed CO [57, 58] or such species as CHO, CH_2, CH, COH, or even C radicals [49, 52, 53, 56]. Additionally, geminal CO adsorbates (i.e., two CO molecules linearly bonded to one surface site) were observed on the electrochemically modified Rh electrodes [60]. It should be added that the product of CO_2/CO adsorption on Rh is regarded as generally more reduced than on Pt [49, 52, 53, 56–58]. On Pd, the product of CO adsorption consists mainly of linearly and bridge-bonded CO, possibly with the addition of a more reduced form [55, 64]. For alloys, it has been found that the structure and composition of CO_2/CO adsorption products are dependent on the surface composition [5, 10, 14].

Recently, we have reported on hydrogen electrosorption into Pd–Rh alloys [41]. In this paper we present the results of studies on selected aspects of the electrochemical behavior of Pd–Rh binary alloy electrodeposits of rough surfaces. We describe some general electrochemical properties of Pd–Rh alloys under conditions of cyclic voltammetric experiments and show the comparative data concerning carbon oxides adsorption on Pd–Rh electrodes for a wide range of alloy compositions. In particular, we have been interested in the possible similarities and differences in CO_2 and CO adsorption products on Pd–Rh alloys.

Experimental

Pd–Rh alloys were prepared by potentiostatic deposition on gold wires (99.9%, 0.5 mm in diameter) from baths containing 0.4 M $RhCl_3$ + 0.022 M $PdCl_2$ + 0.2 M HCl or 0.014 M $RhCl_3$ + 0.024 M $PdCl_2$ + 0.22 M HCl. The electrolysis time was in the range of 400–1,000 s. The higher the potential was, the longer the time necessary for the deposition of a layer of a given thickness was, because a higher potential resulted in a lower current density. Different alloy compositions were obtained applying different deposition potentials (see Fig. 1). For Pd-rich alloys, bulk and surface compositions of freshly prepared electrodes were similar, but for alloys containing more than ca. 20% Rh in the bulk, the surface was strongly enriched with Rh (Fig. 2). Therefore, the preparation of Pd–Rh alloys of bulk compositions between 0 and 50% Rh covered practically the whole spectrum of surface compositions. The significant disagreement between surface and bulk composition of the alloys at higher Rh content probably results

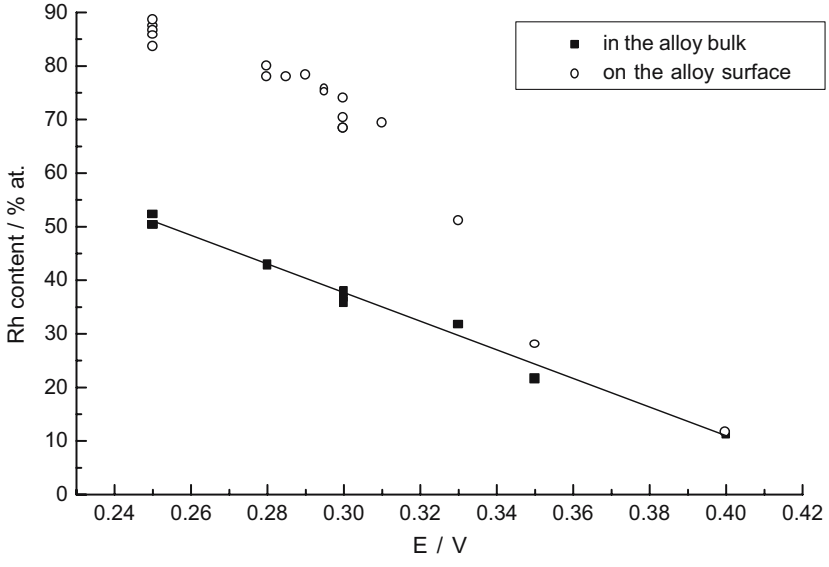

Fig. 1 The dependence of bulk and surface composition of Pd–Rh alloys on the deposition potential during electrolysis from a bath containing 0.4 M $RhCl_3$ + 0.022 M $PdCl_2$ + 0.2 M HCl

from the continuous changes in metal concentration with the progress of the electrodeposition process. It is also likely that electrolyte components in the double layer present at the metal–solution interface interact with Pd and Rh atoms, leading to alloy surface enrichment with one of the metals. However, regardless of the possible inhomogeneity of the alloy bulk due to the preparation method resulting in certain composition differences between particular atomic layers, the surface state was always well defined, as can be judged from the course of cyclic voltammetric curves recorded for freshly prepared Pd–Rh electrodes (see Fig. 3 below). Various surface compositions could also be obtained by controlled potential cycling of freshly prepared electrodes (see "General cyclic voltammetric behavior of Pd–Rh alloys"). The thickness of the deposited alloy layers was of the order of microns (0.5–0.8 μm). The roughness factor of the deposits, as estimated from surface oxide reduction charge measurements [1] (using a conversion factor 424 μC cm^{-2} for reduction of a monolayer of surface oxide), was in the range of 100–350. Bulk compositions of the alloys were determined by an energy dispersive X-ray analysis (EDAX) analyzer (EDR-286) coupled with a LEO 435VP scanning electron microscope (SEM). Surface compositions were determined using the literature method [1, 2] based on a linear dependence of the potential of surface oxide reduction peak on the surface content of an alloy component. A calibration curve for such calculations was constructed using the values of the potential of the aforementioned peak on pure metals, obtained from cyclic voltammograms for Pd and Rh recorded under identical experimental conditions as for alloys. All alloy compositions given in this work are expressed in atomic percentages.

All experiments were performed at room temperature in 0.5 M H_2SO_4 solution deoxygenated using an Ar stream. A three-electrode cell was used with $Hg|Hg_2SO_4|0.5$ M H_2SO_4 as the reference electrode and a Pt gauze as the auxiliary electrode. All potentials are recalculated with respect to the standard hydrogen electrode.

In CO_2 and CO adsorption experiments, the solution was saturated with 99.9% purity gas at a potential from the hydrogen region. After completing the adsorption, which took 45 min for CO_2 and 20 min for CO, the gas was always removed from the solution with Ar and a voltammogram was recorded at a scan rate 0.05 V s^{-1}.

Results and discussion

General cyclic voltammetric behavior of Pd–Rh alloys

Figure 3a–f present cyclic voltammograms recorded for Pd, Rh, and Pd–Rh alloys of different bulk and surface compositions. One can distinguish hydrogen adsorption (1) and desorption (1′) signals (the hydrogen region), then a potential range free from faradaic processes (the double-layer region—2), followed by surface oxide formation (3) and reduction (3′) currents (the oxygen region). Due to the presence of Pd, the alloys can also absorb hydrogen [38–42], which is mirrored by the presence of additional current signals due to electrochemical hydrogen insertion (1a) and removal (1a′).

The double-layer region is more pronounced for alloys rich in Pd, while for Rh and Rh-rich alloys in region (2) there is an overlapping of hydrogen desorption signals and surface oxidation currents. In the oxygen region, one should note various potentials of the onset of the processes of surface oxidation (oxygen adsorption) and surface oxide reduction (oxygen desorption). Interestingly, in the case of Rh-rich Pd–Rh alloys, the process of surface oxide formation happened to begin at a potential as low as that for pure Rh. The enrichment of the alloy surface with Pd results in the onset of surface oxide formation and reduction shifted to higher potentials. As it can be seen in Fig. 3, a single peak of surface oxide reduction (3′) was observed for all freshly prepared Pd–Rh electrodes independently of bulk and surface composition, indicating phase homogeneity of the alloy surface [1].

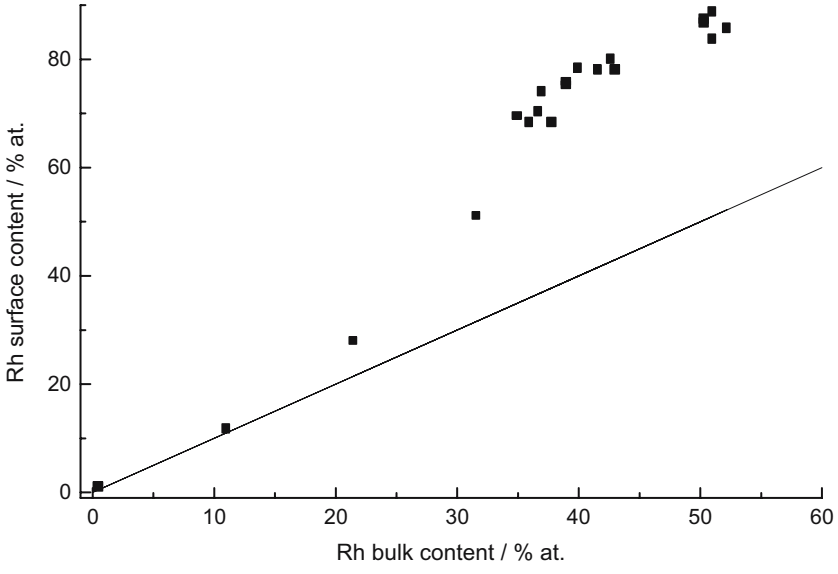

Fig. 2 Surface composition as a function of bulk composition for freshly deposited Pd–Rh alloys

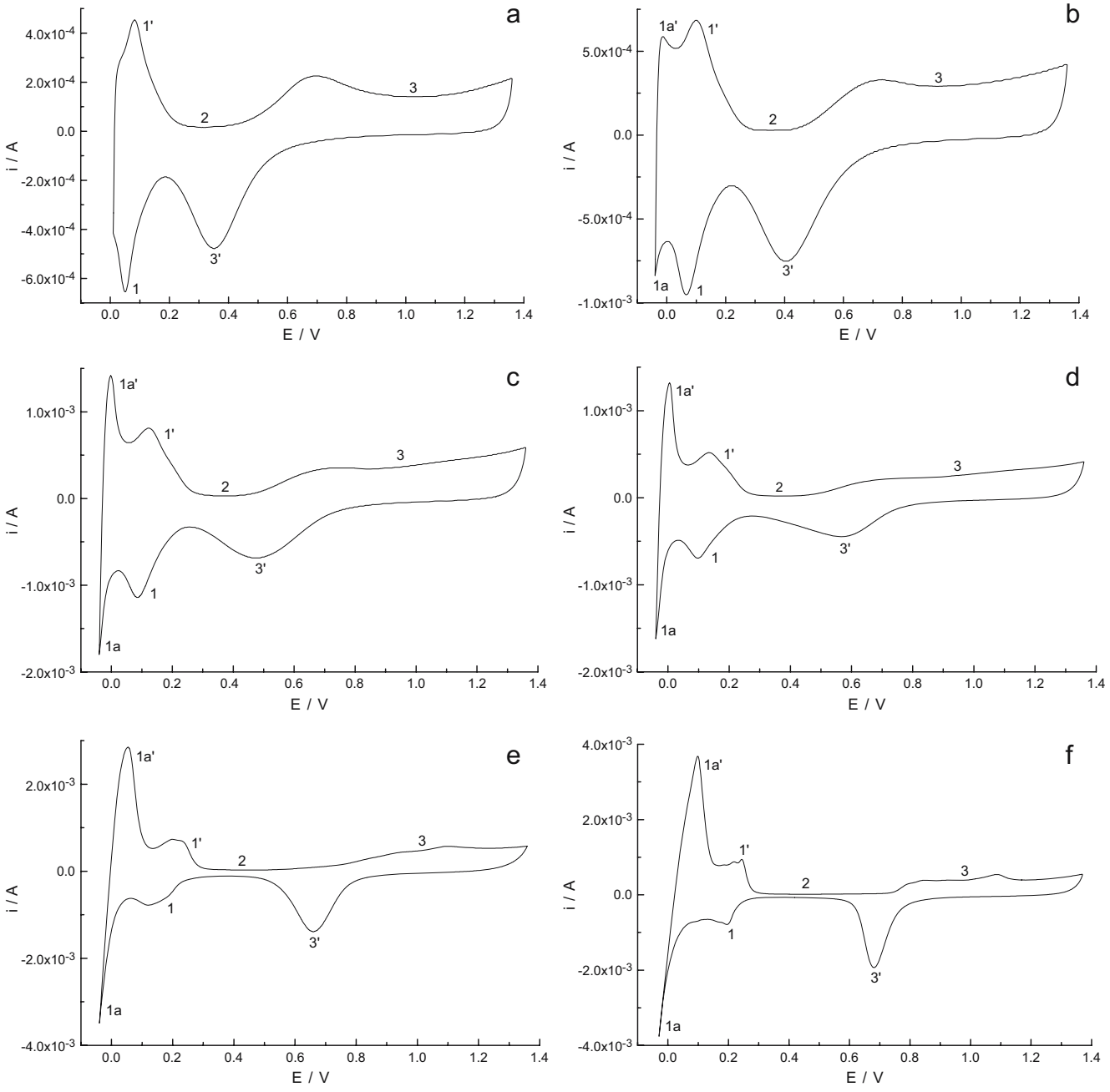

Fig. 3 Cyclic voltammograms for Pd, Rh, and Pd–Rh alloys recorded in the hydrogen–oxygen potential range (from −0.04 to 1.36 V), scan rate of 0.05 V s^{-1}: **a** pure Rh; **b** Pd–Rh alloy, 51% Rh bulk, 83% Rh surface; **c** Pd–Rh alloy, 36% Rh bulk, 63% Rh surface; **d** Pd–Rh alloy, 32% Rh bulk, 37% Rh surface; **e** Pd–Rh alloy, 11% Rh bulk, 10% Rh surface; **f** pure Pd

It should be emphasized that the cyclic voltammetry technique seems to be the most appropriate method for in situ investigations of the electrochemistry of such systems. Some techniques useful in surface investigations, like X-ray photoelectron spectroscopy, Auger electron spectroscopy, ion scattering spectroscopy, and secondary ion mass spectrometry, are ex situ techniques and they cannot provide results concerning the surface state of the electrode in the solution and subjected to polarization. As it was established during electrochemical studying on pure noble metals and their binary alloys [1–37], a cyclic voltammetric curve could be treated as a basic means of characterizing and analyzing the surfaces of electrodes of this type. The voltammogram recorded under given experimental conditions is characteristic of the individual noble metal and it is an electrochemical "fingerprint" of the investigated sample. Thus, we can draw qualitative and quantitative conclusions about the surface state of binary Pd–Rh alloys on the basis of the course of cyclic voltammetric curves by utilizing the distinctive features associated with each component. Such an analysis is possible, owing to the fact that the voltammograms for pure Pd and Rh electrodes

differ markedly from each other in respect to the region of surface oxide formation and reduction, as well as the appearance of the region where hydrogen electrosorption takes place [1, 2]. Figure 3 clearly demonstrates that with the change in alloy composition the voltammogram shape transforms from a cyclic voltammetric curve typical of Rh into that characteristic of Pd.

As reported in earlier papers [1, 2, 4, 8, 19–25, 27, 28, 31, 34, 36, 65], long potential cycling of noble metal alloys involving polarization to the oxygen region causes significant changes in the surface state of the electrode, resulting from electrochemical dissolution of the alloy components. These changes are reflected in the voltammogram course and are observed for both oxygen and hydrogen signals. This course is illustrated in Fig. 4 presenting a series of cyclic voltammetric curves recorded for a Pd–Rh alloy (containing initially 47% Rh in the bulk and 87% Rh on the surface) subjected to electrochemical aging, i.e., cycling in the hydrogen–oxygen potential range (from −0.04 to 1.36 V, scan rate 0.1 V s^{-1}).

It should be noted that at the beginning of the cycling procedure, the potential of the surface oxide reduction peak (3′) is not altered, suggesting constant surface composition despite both Rh and Pd dissolution, as expected on the basis of the literature data [44]. Such a steady state can be explained assuming that the ratio between the dissolution rates of Rh and Pd is similar to their relative surface content [2]. However, long potential cycling (175–200 cycles) causes the splitting of the surface oxide reduction peak into two signals (insert a in Fig. 4). This splitting indicates that the surface of Pd–Rh alloys becomes heterogeneous [1], i.e., a separation occurs into two surface phases of different compositions, namely, one rich in Rh and one rich in Pd. The mechanism of this segregation might involve a partial cathodic redeposition of previously dissolved metals in proportions different than that for dissolution. Moreover, the Pd–Rh system is not expected to be homogeneous over the whole composition range [2]. During further potential cycling, the initial peak disappears and the surface becomes, again, homogeneous, but strongly enriched with Pd, as can be concluded from the voltammogram shape (insert b in Fig. 4). It should be pointed out that the process described above could be facilitated by the fact that the surface of the fresh alloy investigated was strongly enriched with Rh. Such surface arrangement is energetically unfavorable because, under conditions of minimum surface energy, the stable surface of binary Pd–Rh alloys is enriched with Pd [66, 67]. In contrast to the Pd–Rh system, surface modifications leading to alloy heterogeneity were not observed in the case of Pt–Rh alloys subjected to the same procedure, where a continuous shift of the potential of the surface oxide reduction peak was observed, indicating continuous changes in composition of a single alloy surface phase [2, 8]. Similar behavior was observed here for a Pd–Rh electrode initially less rich in Rh (37% in the bulk, 70% on the surface) than the previous one. In the case of the electrode less rich in Rh, the electrode surface remained homogeneous during its progressive enrichment with Pd.

The comparison of the compositions before and after the potential cycling (see Table 1) showed that such electrochemical treatment produced Pd–Rh alloys enriched with Pd at the expense of Rh. Because significant changes in composition can be detected by EDAX technique, examining thicknesses of the order of thousand atomic layers, it means that the metals are removed not only from the

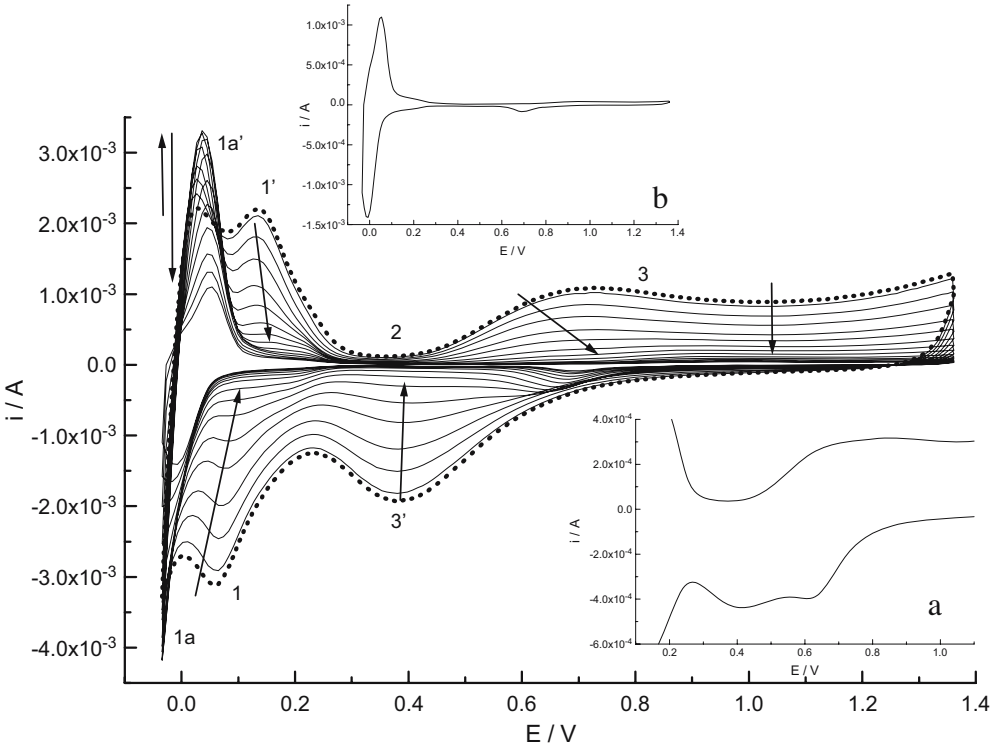

Fig. 4 Cyclic voltammograms for a Pd–Rh alloy (initial composition: 47% Rh in the bulk and 87% Rh on the surface) recorded during continuous potential cycling in the hydrogen–oxygen potential range (from −0.04 to 1.36 V), scan rate of 0.1 V s^{-1} (every 25th cycle is shown). First scan is indicated by a *dotted line*. *Arrows* show changes in current. Inserts: **a** cyclic voltammogram after 180 cycles, **b** cyclic voltammogram after 450 cycles

surface but also from the bulk of the alloy (at least from some layers close to the surface). Because of a small electrode thickness, the region involved with composition changes might be relatively large with respect to the sample volume. The composition changes detected by EDAX measurements indicate that the process of metal redeposition is limited and a predominant part of the metal is irreversibly removed from the electrode.

The effect of composition changes occurs simultaneously with the decrease in the real surface area of the electrode indicated by the decrease in hydrogen adsorption/desorption (signal 1 and 1′), as well as oxide formation and reduction currents (3 and 3′). As it was reported in the literature [68, 69], the surface roughness of noble metal electrodes subjected to the procedure of potential cycling through the oxygen region may increase or decrease, and the tendency depends on the parameters applied in a cyclic voltammetric experiment. In our experiments the latter case takes place, which is consistent with the results reported earlier for Pd–Au [23], Pt–Au [31], and Pd–Pt–Rh alloys [65] under similar conditions.

The tendency of a monotonic current decrease is exhibited by all signals, with the exception of the peaks 1a and 1a′ (see Fig. 4) originating mainly from hydrogen absorption and removal. At the beginning of potential cycling these signals increase, indicating the rise in the alloy's ability to absorb hydrogen, which is in line with EDAX results showing the enrichment of alloy with Pd. These composition changes could facilitate hydrogen absorption in the alloy both kinetically—by removing from the surface Rh atoms, and therefore improving the surface stage of hydrogen insertion into alloy bulk proceeding via Pd surface centers—and thermodynamically—by removing Rh from the bulk and producing an alloy containing more Pd, i.e., absorbing more hydrogen. Further lowering of hydrogen absorption signals can be explained by the progressive diminution of the thickness of the hydrogen-absorbing layer caused by metal dissolution.

SEM images (Fig. 5) confirm the alteration of the alloy surface during the potential cycling procedure. As can be seen in Fig. 5, we observe changes in crystallites sizes, and consequently, in the surface roughness, as a result of the surface oxide formation/reduction processes accompanied by metal dissolution and subsequent partial redeposition. Besides, because for Pd and Pd alloys the lattice parameter increases due to the formation of the hydride phase [40, 42], hydrogen penetration into the bulk of the electrode causes an increase in sample volume leading to cracking.

Carbon oxides adsorption on Pd–Rh alloys

Carbon oxides adsorption was performed on Pd–Rh alloys at potentials of hydrogen adsorption for a wide range of surface compositions. In contrast to the Pt–Rh system [5, 10], where both elements are active in CO_2 adsorption and the reaction proceeds for the full composition spectrum, in the Pd–Rh system the decrease in surface Rh content markedly weakens the alloy affinity to CO_2, because hydrogen adsorbed on Pd atoms does not take part in the reaction with CO_2 molecules [54, 55]. For Pd-rich Pd–Rh alloys, containing less than ca. 20% Rh on the surface, the amount of adsorbed CO_2 was negligible. On the other hand, CO can be adsorbed on both metals [50, 55] and, therefore, also on their alloy, regardless of its composition.

Figure 6 presents anodic parts of voltammograms recorded after CO_2 (solid line) and CO adsorption (dashed line) together with a blank curve (dotted line) recorded in the absence of the adsorbate for a Pd–Rh alloy containing 39% Rh in the bulk and 72% Rh on the surface. The main features of the voltammograms recorded in the presence of the adsorption product are: (1) a decrease in hydrogen oxidation currents reflecting blocking hydrogen adsorption reaction on surface sites occupied by adsorbed CO_2 or CO and (2) a peak of the adsorbate oxidation, placed at potentials in the oxygen region.

The influence of the presence of adsorbed CO_2 and CO on hydrogen signals is different for both adsorbates. The peak at higher potentials originating mainly from the oxidation of adsorbed hydrogen is significantly decreased in the presence of adsorbed CO_2, while the peak placed at lower potentials, attributed mainly to the oxidation of absorbed hydrogen, is less affected by adsorbed CO_2. The little influence of the presence of adsorbed CO_2 on the processes of hydrogen absorption and its removal from the alloy bulk has been demonstrated in recent reports [14, 70]. On the other hand, adsorbed CO causes strong suppression of both hydrogen peaks, which means that this adsorbate creates a barrier not only for hydrogen adsorption but also for hydrogen absorption.

The general shape and potential of the oxidation peaks of adsorbed CO_2 and CO are different. A flat and broad peak of adsorbed CO_2 oxidation is always placed at a potential

Table 1 Bulk and surface compositions of fresh and aged Pd–Rh alloys

Sample	Alloy thickness (μm)	Electrode state	Bulk composition		Surface composition	
			at.% Pd	at.% Rh	at.% Pd	at.% Rh
1	0.79	Fresh electrode	53	47	13	87
		After 450 cycles	71	29	98	2
2	0.63	Fresh electrode	59	41	15	85
		After 600 cycles	90	10	96	4
3	0.74	Fresh electrode	63	37	30	70
		After 230 cycles	83	17	90	10

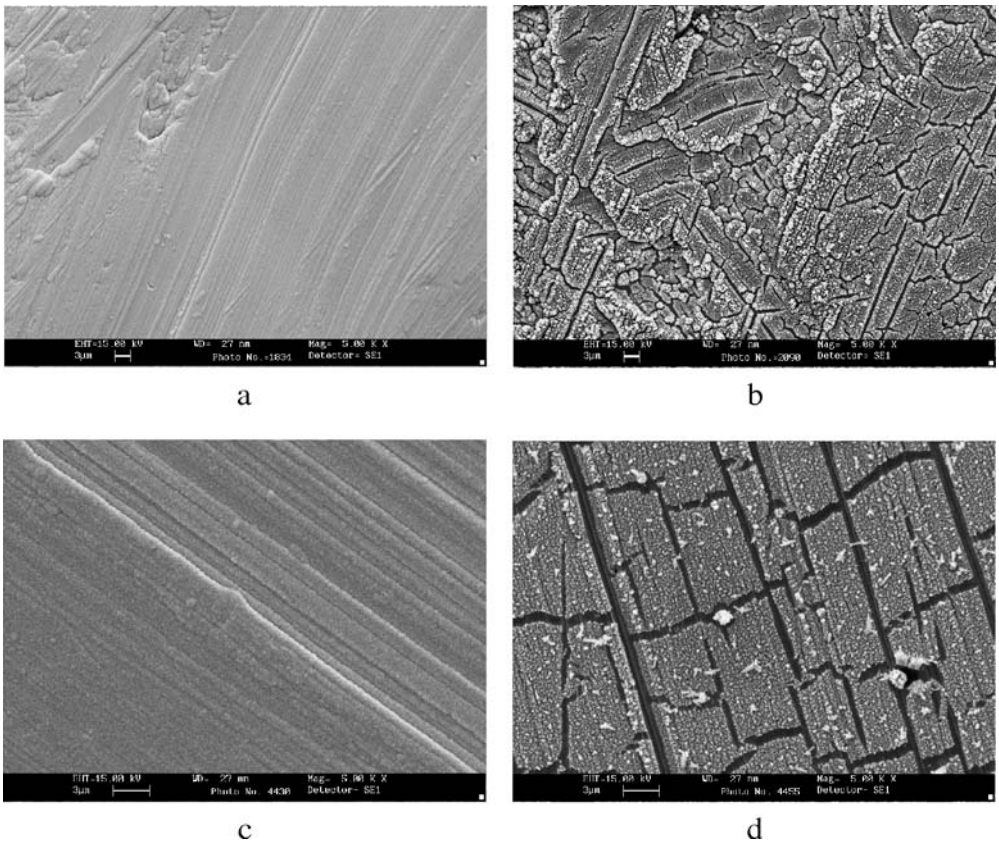

Fig. 5 SEM images taken for Pd-Rh alloys: a fresh alloy containing 47% Rh in the bulk and 87% Rh on the surface (**a**) and after 450 cycles (**b**); a fresh alloy containing 37% Rh in the bulk and 70% Rh on the surface (**c**) and after 230 cycles (**d**). Potential cycling range from −0.04 to 1.36 V; scan rate 0.1 V s^{-1}

higher than that corresponding to the onset of surface oxidation, and its descending part extends far into the oxygen region. The peak of CO oxidation is much sharper than in the case of CO_2 and is placed at a higher potential. For both adsorbates the peaks of their oxidation are shifted into higher potentials with the decrease in Rh surface concentration (see Fig. 7). This is again in contrast to the situation for Pt–Rh alloys where, for certain compositions, the oxidation of adsorbed CO_2 occurred at potentials markedly lower than on pure metals [10].

In the case of Pd–Rh alloys of Rh surface content higher than ca. 70%, the surface state was unstable, as could be concluded from changes in the surface oxide reduction peak observed during CO_2 and CO adsorption experiments. As can be seen in Fig. 8, after the adsorption procedure, not only the peak of surface oxide reduction but also the onset of surface oxidation was shifted into lower potentials by several millivolts. This might mirror the modifications of surface composition resulting from the interactions of Pd and Rh atoms with CO_2 or CO molecules, which lead to the surface enrichment with the

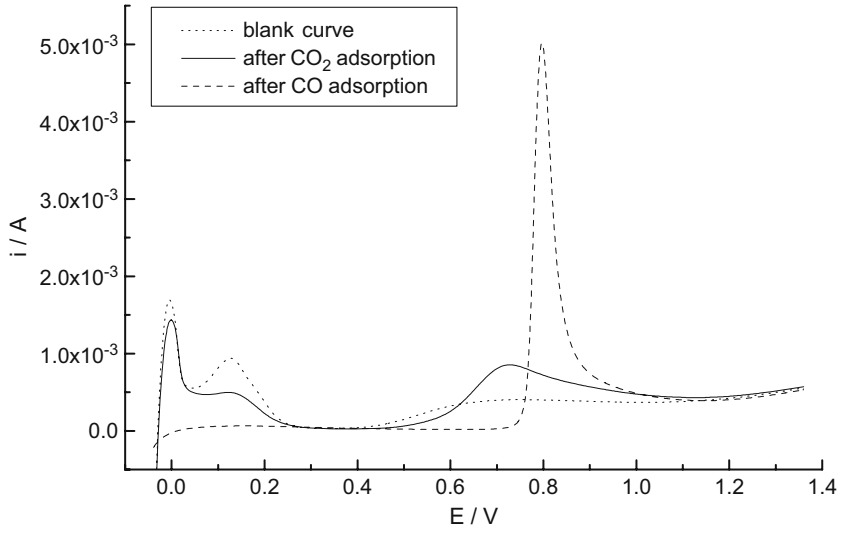

Fig. 6 Anodic parts of cyclic voltammograms (scan rate 0.05 V s^{-1}) recorded after CO_2 adsorption 45 min at 0.06 V (*solid line*), after CO adsorption 20 min at 0.06 V (*dashed line*), and without CO_2/CO—blank curve (*dotted line*)—for a Pd–Rh alloy (39% Rh in the bulk and 72% Rh on the surface)

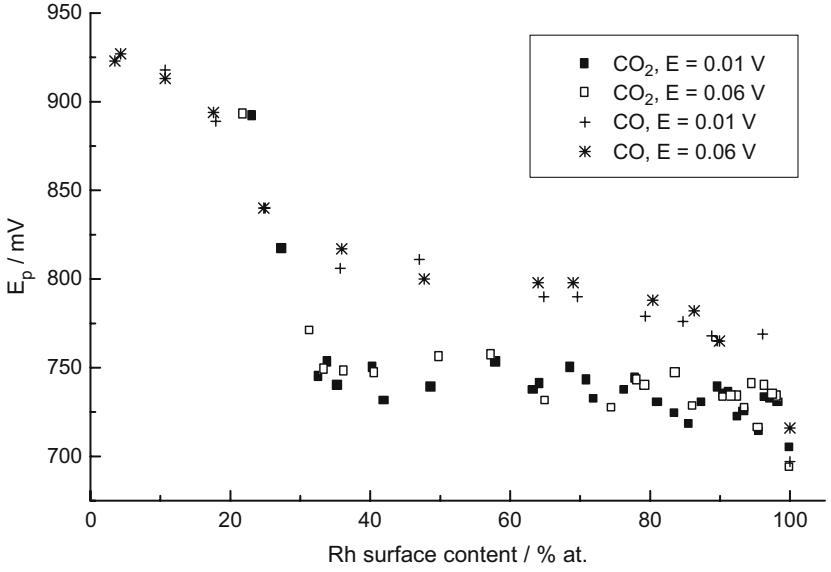

Fig. 7 The influence of Rh surface concentration on the potential of the oxidation peak of adsorbed CO_2 and CO on Pd–Rh alloys for two adsorption potentials (0.01 and 0.06 V); scan rate during adsorbate oxidation is 0.05 V s^{-1}

alloy component of a greater affinity to the adsorbate, i.e., Rh, as can be concluded from a negative potential shift. A typical enrichment was ca. 10%. It should be stressed that the shift of the peak was observed only after the first adsorption run on a given electrode, and further CO_2 or CO adsorption did not cause any additional effects. The possibility that this was the result of the interactions of the alloy surface with hydrogen (an effect reported for Pd–Au alloys [23]) was excluded because prolonged electrode polarization in the hydrogen region in the absence of carbon oxides in the solution did not change the position of the surface oxide reduction peak.

On the basis on the voltammetric signals it is possible to calculate the electron per site (eps) value, i.e., a number of electrons taking part in the process of the adsorbate oxidation from one surface site. This quantity can be obtained from the ratio of the adsorbate oxidation charge (Q^{ox}_{COx}) to the difference between the charges of adsorbed hydrogen oxidation (calculated from the area under peak 1′) in the absence and presence of the adsorbate (ΔQ^{ox}_{Hads}):

$$eps = Q^{ox}_{COx} / \Delta Q^{ox}_{Hads} \quad (1)$$

Figure 9 presents eps values plotted against Rh surface concentration for CO_2 and CO adsorption on Pd–Rh alloys. In general the values are not integers, indicating a mixed nature of the adsorbate, composed at least of two kinds of species of different eps values. In the case of eps values between 1 and 2, the products of CO_2 and CO adsorption can be linearly (eps=2) and bridge-bonded (eps=1) CO molecules in various relative amounts. When eps is higher than 2, additional products might be proposed, such as multibonded C—H or C—OH species, suggested earlier for Rh electrodes [49, 52, 53, 56]. It should be stressed that due to the strong acidity of the solutions used in our experiments (0.5 M H_2SO_4), the possibility of carbonate formation from dissolved CO_2 can be excluded.

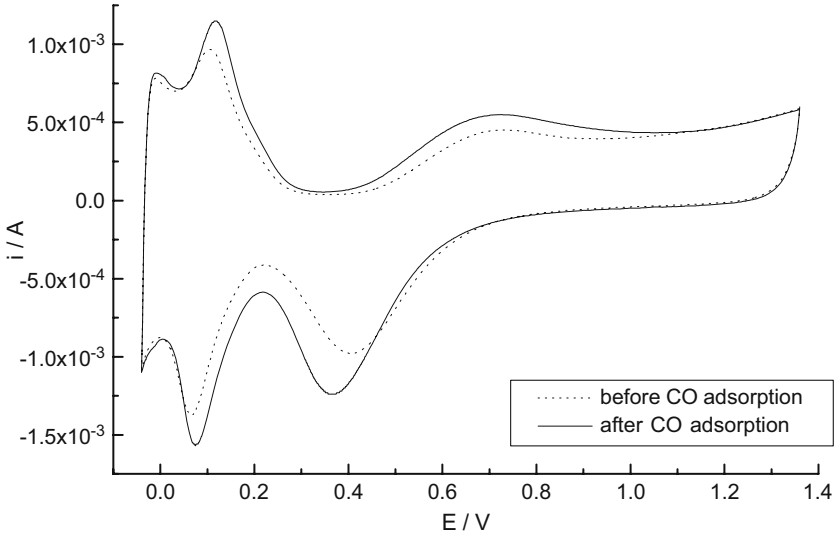

Fig. 8 Cyclic voltammograms (scan rate of 0.05 V s^{-1}) before (*dotted line*) and after (*solid line*) CO adsorption on a Pd–Rh alloy containing in the bulk 50% Rh. Surface composition: initially—83% Rh, after CO adsorption—95% Rh. Adsorption potential of 0.01 V, time of 20 min

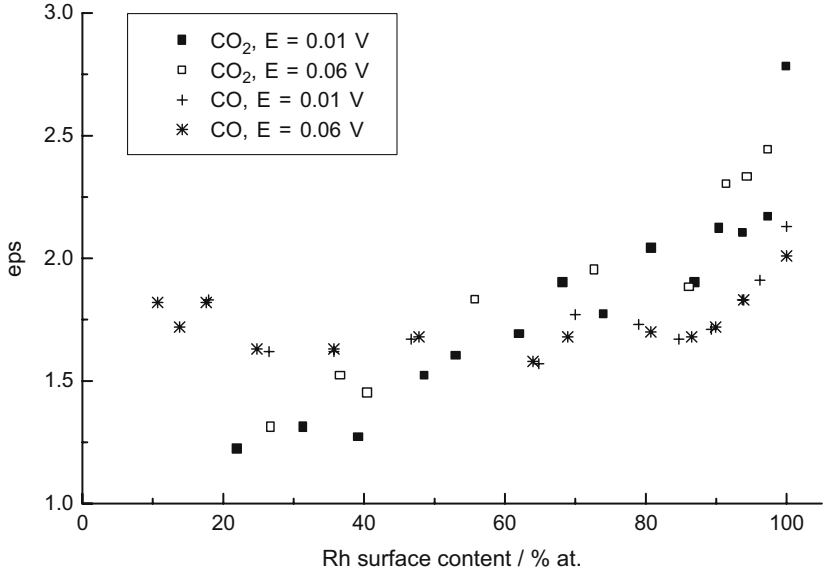

Fig. 9 The influence of Rh surface concentration on the eps values calculated for CO_2 and CO adsorption on Pd–Rh alloys for two adsorption potentials (0.01 and 0.06 V); scan rate during adsorbate oxidation is 0.05 V s^{-1}

Figure 9 demonstrates that the alloy surface composition affects the eps value, and therefore, the nature of the adsorbate. For both carbon oxides, eps values are the highest for pure Rh and decrease when Rh is alloying with Pd. It should be noted that the general course of the dependence of eps on alloy surface concentration is different for CO_2 and CO. In the case of CO_2, adsorption eps values markedly decrease with the decline of Rh content, while for CO adsorption they are practically constant for a wide composition range. This quantitative difference might reflect a qualitatively different nature of the adsorbate. Such behavior is possible due to the fact that in the Pd–Rh system, both components can adsorb CO, while only Rh is active in CO_2 adsorption. Interestingly, the changes in eps values with Pd content suggest that, despite the inertness of Pd atoms in CO_2 adsorption reaction, their presence on the electrode surface affects the behavior of CO_2 molecules towards Rh atoms in the Pd–Rh alloy.

As it is demonstrated in Figs. 7 and 9, there is only little influence of the adsorption potential on the values of the potential of the adsorbate oxidation peak and eps for a given carbon oxide. On the other hand, some differences in the electrochemical behavior are observed between CO_2 and CO adsorption products formed at a given adsorption potential. The comparison of voltammogram shapes and eps values suggests that the products of CO_2 and CO adsorption on Pd–Rh alloys are similar but not totally identical. The differences in the processes of CO_2 and CO adsorption on Rh electrodes were suggested in earlier reports [52, 53]. It is possible that the adsorbates consist of two or more kinds of species of different ratios. The similarity of eps values for some alloy compositions might indicate that the major products of CO_2 and CO adsorption are the same (linearly and bridge-bonded CO species in various relative amounts) but the constitution of minor products is probably different.

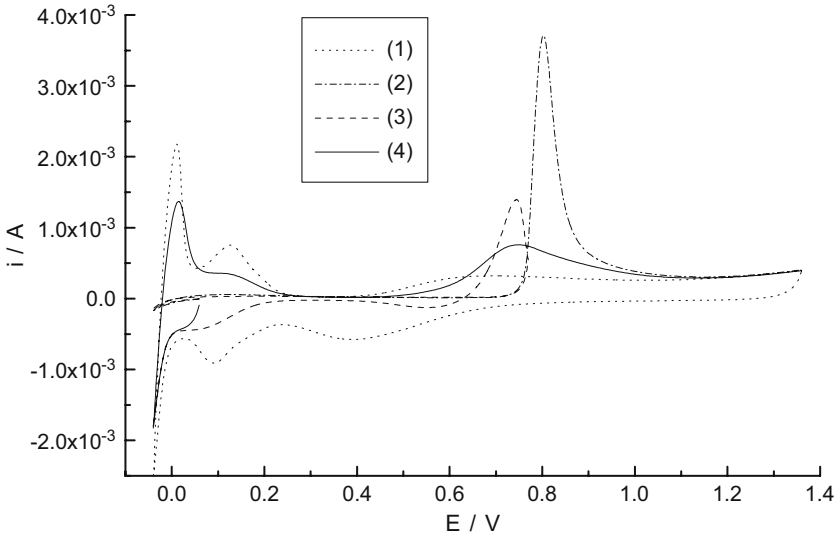

Fig. 10 Cyclic voltammograms (scan rate 0.05 V s^{-1}) recorded after CO adsorption 20 min at 0.06 V on a Pd–Rh alloy (40% Rh in the bulk and 88% Rh on the surface): *1* blank curve, *2* oxidation of adsorbed CO in a full potential range, *3* partial oxidation of adsorbed CO in a limited potential range, *4* oxidation of the remaining part of adsorbed CO after its partial oxidation in procedure (3)

The above statements seem to be confirmed in an experiment where adsorbed CO was oxidized in two steps. After partial removal of the adsorbate by its incomplete oxidation in a limited potential range, the remaining amount was oxidized in a full potential range. As it can be seen in Fig. 10, the voltammogram (curve 4) resembles that typical for CO_2 oxidation (compare with Fig. 6). This means that after the removal of the more easily oxidizable part of CO adsorption products, the remaining species behave very similar to CO_2 adsorption products. This might suggest that among CO adsorption products there are the same species, which are also in CO_2 adsorption products. It is possible that surface centers occupied by adsorbed CO_2 and CO are not the same. Some amount of adsorbed CO might occupy additional sites which are energetically less favorable than the main sites occupied by the rest of the CO and CO_2 adsorption products. It should be stressed that these two kinds of surface sites should not be identified with two alloy components (Pd and Rh atoms) because a similar effect was also observed on pure Rh.

Conclusions

Cyclic voltammograms for Pd–Rh alloys are intermediate between cyclic voltammetric curves for Pd and Rh with well-defined hydrogen electrosorption (adsorption, absorption, and desorption) peaks, as well as surface oxide formation and reduction signals.

As a result of prolonged potential cycling of Pd–Rh alloys through the oxygen region, both electrode surface and bulk are enriched with Pd. During the procedure of electrochemical aging, the surface can become temporarily heterogeneous.

Adsorbed CO_2 causes a diminution of currents originating from hydrogen adsorption on Pd–Rh alloys, but it has much less influence on signals connected with hydrogen absorption. In the presence of adsorbed CO, both hydrogen adsorption and absorption currents are strongly suppressed.

The potentials of the oxidation peaks of adsorbed CO_2 and CO, as well as the number of electrons required for the oxidation of the adsorbate from one surface site (eps), depend on the alloy surface composition. The changes in Rh surface content influence the eps values for CO_2 adsorption more than for CO adsorption. The comparison of voltammogram shapes and eps values suggests that the products of CO_2 and CO adsorption on Pd–Rh alloys are similar, but not totally identical.

Acknowledgements This work was partially financially supported by the Department of Chemistry of Warsaw University and the Industrial Chemistry Research Institute.

References

1. Woods R (1976) In: Bard AJ (ed) Electroanalytical chemistry, vol 9. Marcel Dekker, New York, p 2
2. Rand DAJ, Woods R (1972) J Electroanal Chem 36:57
3. Rand DAJ, Woods R (1974) Surf Sci 41:611
4. Mayell JS, Barber WA (1969) J Electrochem Soc 116:1333
5. Czerwiński A, Sobkowski J (1984) Anal Lett 17:2175
6. Czerwiński A, Marassi R, Sobkowski J (1984) Ann Chim 74:681
7. Poirier JA, Stoner GE (1995) J Electrochem Soc 142:1127
8. Baker BG, Rand DAJ, Woods R (1979) J Electroanal Chem 97:189
9. Aston MK, Rand DAJ, Woods R (1984) J Electroanal Chem 163:199
10. Siwek H, Łukaszewski M, Czerwiński A (2004) Pol J Chem 78:1121
11. Quiroz MA, Gonzalez I, Meas Y, Lamy-Pitara E, Barbier J (1987) Electrochim Acta 32:289
12. Kabbabi A, Faure R, Durand R, Beden B, Hahn F, Leger J-M, Lamy C (1998) J Electroanal Chem 444:41
13. López de Mishima BA, Mishima HT, Castro G (1995) Electrochim Acta 40:2491
14. Grdeń M, Paruszewska A, Czerwiński A (2001) J Electroanal Chem 502:91
15. Grdeń M, Piaścik A, Koczorowski Z, Czerwiński A (2002) J Electroanal Chem 532:35
16. Capon A, Parsons R (1975) J Electroanal Chem 65:285
17. Kadirgan F, Beden B, Leger J-M, Lamy C (1981) J Electroanal Chem 125:89
18. Dalbay N, Kadirgan F (1991) Electrochim Acta 36:353
19. Guerin S, Attard GS (2001) Electrochem Commun 3:544
20. Solla-Gullón J, Montiel V, Aldaz A, Clavilier J (2002) Electrochem Commun 4:716
21. Conway BE, Angerstein-Kozlowska H, Czartoryska G (1978) Z Phys Chem N F 112:195
22. Łukaszewski M, Kuśmierczyk K, Kotowski J, Siwek H, Czerwiński A (2003) J Solid State Electrochem 7:69
23. Łukaszewski M, Czerwiński A (2003) Electrochim Acta 48:2435
24. Beden B, Lamy C, Leger J-M (1979) Electrochim Acta 24:1157
25. Woods R (1969) Electrochim Acta 14:632
26. Gossner K, Mizera E (1981) J Electroanal Chem 125:359
27. Gossner K, Mizera E (1982) J Electroanal Chem 140:47
28. Nishimura K, Machida K, Enyo M (1988) J Electroanal Chem 257:217
29. Nishimura K, Machida K, Enyo M (1988) J Electroanal Chem 251:103
30. Enyo M (1985) J Electroanal Chem 186:155
31. Kuśmierczyk K, Łukaszewski M, Rogulski Z, Siwek H, Kotowski J, Czerwiński A (2002) Pol J Chem 76:607
32. Breiter MW (1965) J Phys Chem 69:901
33. Breiter MW (1965) Electrochim Acta 10:543
34. Woods R (1969) Electrochim Acta 14:533
35. Woods R (1971) Electrochim Acta 16:655
36. Rach E, Heitbaum J (1987) Electrochim Acta 32:1173
37. Möller H, Pistorius PC (2004) J Electroanal Chem 570:243
38. Barton JC, Green JAS, Lewis FA (1966) Trans Faraday Soc 62:960
39. Lewis FA, McFall WD, Witherspoon TC (1973) Z Physik Chem N F 84:31
40. Sakamoto Y, Haraguchi Y, Ura M, Chen FL (1994) Ber Bunsenges Phys Chem 98:964
41. Żurowski A, Łukaszewski M, Czerwiński A (2006) Electrochim Acta (in press)
42. Lewis FA (1967) The palladium–hydrogen system. Academic, London
43. Jerkiewicz G (1998) Prog Surf Sci 57:137
44. Rand DAJ, Woods R (1972) J Electroanal Chem 35:209
45. Jerkiewicz G (1999) In: Wieckowski A (ed) Interfacial electrochemistry. Marcel Dekker, New York, p 559
46. Conway BE (1995) Prog Surf Sci 49:331
47. Czerwiński A, Sobkowski J, Więckowski A (1974) Int J Appl Radiat Isot 25:295
48. Sobkowski J, Czerwiński A (1974) J Electroanal Chem 55:391
49. Sobkowski J, Więckowski A, Zelenay P, Czerwiński A (1979) J Electroanal Chem 100:781

50. Breiter MW (1984) J Electroanal Chem 180:25
51. Czerwiński A, Sobkowski J (1978) J Electroanal Chem 91:47
52. Czerwiński A, Sobkowski J, Kaczmarek A, Nowakowska M (1985) Anal Lett 18:1465
53. Czerwiński A (1988) J Electroanal Chem 252:189
54. Vassilev YB, Bagotzky VS, Osetrova NV, Mikhailova AA (1985) J Electroanal Chem 189:311
55. Czerwiński A (1994) J Electroanal Chem 379:487
56. Zakharian AV, Osetrova NV, Vasiliev YB (1976) Electrokhimiya 12:1854
57. Marcos ML, González-Velasco J, Bolzán AE, Arvia AJ (1995) J Electroanal Chem 395:91
58. Arévalo MC, Gomis-Bas C, Hahn F (1998) Electrochim Acta 44:1369
59. Hoshi N, Ito H, Suzuki T, Hori Y (1995) J Electroanal Chem 395:309
60. Lin W-F, Sun S-G (1996) Electrochim Acta 41:803
61. Weaver MJ, Chang SC, Leung LWH, Jiang X, Rubel M, Szklarczyk M, Zurawski D, Wieckowski A (1992) J Electroanal Chem 327:247
62. Gómez R, Rodes A, Pérez JM, Feliu JM, Aldaz A (1995) Surf Sci 327:202
63. Gómez R, Rodes A, Pérez JM, Feliu JM, Aldaz A (1995) Surf Sci 344:85
64. Czerwiński A, Zamponi S, Marassi R (1991) J Electroanal Chem 304:233
65. Łukaszewski M, Grdeń M, Czerwiński A (2005) J Solid State Electrochem 1:9
66. Batirev IG, Leiro JA (1995) J Electron Spectrosc Rel Phen 71:79
67. Leiro JA, Heinonen MH, Batirev IG (1995) Appl Surf Sci 90:515
68. Bolzan A, Martins ME, Arvia AJ (1986) J Electroanal Chem 207:279
69. Perdriel CL, Custidiano E, Arvia AJ (1988) J Electroanal Chem 246:165
70. Łukaszewski M, Grdeń M, Czerwiński A (2004) Electrochim Acta 49:3161